

Wind Induced Fatigue of Flare Booms: Evaluation of Different Methods and Software Alternatives

Ahmed Adel Mohamed Radwan¹, Nikolas Bentzen¹, Ivar Holta¹, Gunnar Gjerde¹ and Sudath C. Siriwardane²

¹ Aker Solutions, Stavanger, Norway

² University of Stavanger, 4036 Stavanger, P.O. box 8600, Norway
sasc.siriwardane@uis.no

Abstract. Wind-induced fatigue is a critical design concern for slender offshore structures such as flare booms. This paper compares two established fatigue assessment approaches: the spectral method implemented in SESAM FRAMEWORK, and the nonlinear time history analysis performed using USFOS. Both rely on the hot spot stress approach and are applied to the same structural model of a North Sea flare boom, using consistent wind loading data derived from the NPD/Frøya spectra. A detailed parametric analysis was conducted to assess the effects of drag coefficient, weight factor, wind block configuration, and relative velocity. Results indicate that FRAMEWORK generally predicts longer fatigue life than USFOS, with an average difference of 66%. Sensitivity to input parameters, such as weight-induced natural frequency shifts and wind block distribution, was also analyzed. While FRAMEWORK offers easier setup and faster computation, USFOS provides more detailed stress histories and better captures nonlinear effects, though at a higher computational cost. The study highlights the need for careful method selection and the importance of validation against real-world data for reliable fatigue assessment.

Keywords: Wind-induced fatigue, flare boom, spectral method, time history analysis, FRAMEWORK, USFOS

1 Introduction

Wind-induced dynamic loading causes structural vibrations that generate fluctuating stresses, leading to fatigue damage and potential failure, often at stress levels well below the material's yield strength. For slender steel structures like offshore flare booms, where fatigue is the dominant design consideration, relying solely on Ultimate Limit State (ULS) is insufficient; instead, the Fatigue Limit State (FLS) is applied to account for high-frequency dynamic loads that take place below the yielding resistance of the material. These structures, composed mainly of tubular members, are prone to high stress concentrations and fatigue cracking at joints. Due to the limitations of finite element modelling and load variability, accurately estimating fatigue life remains challenging. Consequently, reliable computational methods, such as time domain nonlinear

dynamic analysis and the power spectral density approach, both based on the hot spot stress method, are employed in the industry [1, 2].

The frequency domain analysis is a convenient and relatively simple methods, but it has its limitations. Both material and geometrical non-linear effects are some of the factors the method cannot take properly into account. Cross wind induced vibrations, wind directional effects, structural damping and incident turbulence may all effect the bandwidth of the critical stress in the power spectrum, such that the fatigue damage contribution might be underestimated [3].

Time histories is tedious and require a lot of input data. Large statistical variation and difference is also found within one stress recording to the next one. There is therefore a demand for further research and development in more accurate and simpler assessment methods for time history. More accurate spectral approach is also desirable because of the simplicity, but it is necessary to confirm numerical models with real behavior through research [4]. Naess states in their report that time domain fatigue analysis is more accurate than spectral method [5]. However, different standards still rely on spectral method as it is computationally less demanding. On a side note, standards recommend analyzing fatigue using time domain method, when nonlinear analysis is required. Therefore, there is research demand for further development of both methods, especially confirmation with real structural behavior. However, since spectral approaches are generally less demanding, comparing the two methods is also of interest for the practicing industry.

The main objective of this paper is to compare the fatigue assessment results and parametric sensitivity of the two different methods based on a case study. This paper will therefore compare fatigue results from two established software methods for calculating wind induced fatigue on slender structures. One being the method made by DNV using the SESAM software package, specifically FRAMEWORK wind fatigue application, to represent the spectral density approach. To represent the time domain approach, the method established by Junbo Jia on calculating the wind induced fatigue of a typical high rise tubular structure using USFOS [3]. In both cases, the wind loading is based on the NPD/Frøya spectra recommended by API RP 2A-WSD [6].

2 Structural Description of the Case Study Flare Boom

The flare boom considered in this study is taken from an existing offshore platform. It consists of two main components: (i) tubular members and (ii) a supporting structure made of box- and I-section beams forming a box frame, as shown in Fig. 1(a). The supporting structure connects to the platform topside via tubular link members. The base of the flare boom is at an elevation of 24.6 m above sea level (LAT), and its tip reaches 119.8 m. The yield strength, modulus of elasticity, density and Poisson's ratio are 420MPa, 210GPa, 7850kg/m³ and 0.3 respectively. The total weight is 398.15 metric tons, with point masses added to match the target weight and center of gravity. A structural damping ratio of 0.05 is used. To isolate wind effects on the tower, non-tubular members are assumed to be unaffected by wind loading.

Fatigue lives at the five most critical points from each software (FRAMEWORK and USFOS) are used for a parametric comparison. As shown in Fig. 1(b), these points do not correspond directly due to differences in how each software identifies critical nodes. Six nodes are displayed to reflect this variation. Joint numbers differ between the two software: FRAMEWORK uses a six-digit numbering system, while USFOS numbers are shown in parentheses for reference. The S-N curve for tubular members in air (T-curve) is used for all tubular joints, in accordance with DNV-RP-C203 [7].

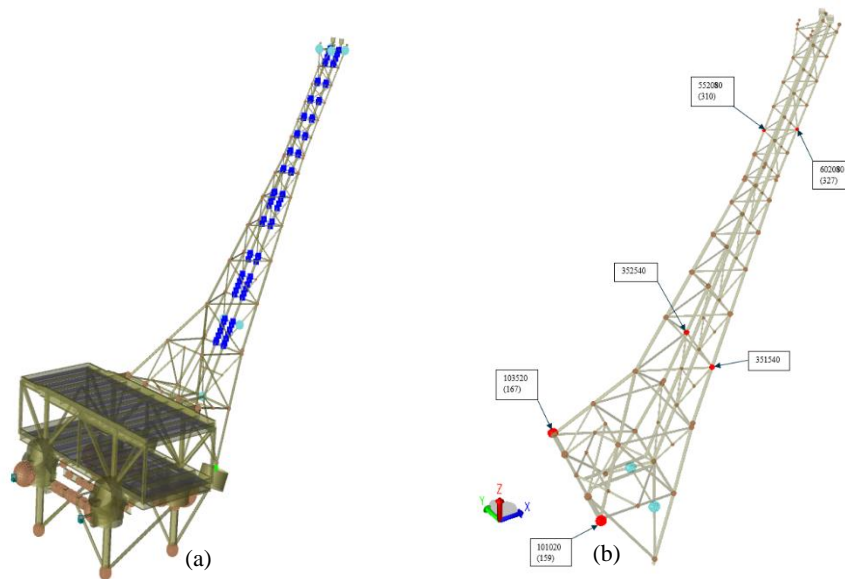


Fig.1. (a). Sesam GeniE Model of the case study flare boom, (b). Isometric view of the model showing critical points

3 Wind Load Simulation

Wind data is extracted from Metocean Design Basis for the corresponding field. This includes the wind profile; all-year wind rose and the scatter diagram. As the all-year wind rose shown in Fig. 2(a), the dominant wind directions are South, South-West and North, respectively. While the least-occurring wind comes from the East direction. Wind profile and gust are based in this Metocean report on the NORSOK Standard [8]. The Fig. 2(b) shows wind profiles for different wind speeds varying with height at the location of interest. Different drag coefficients have been picked for this parametric comparative study. One of the cases is a Reynold's number dependent drag coefficients C_d are 0.65 and 1.2 were taken respectively for larger and lower Reynolds number than 500,000 respectively [1].

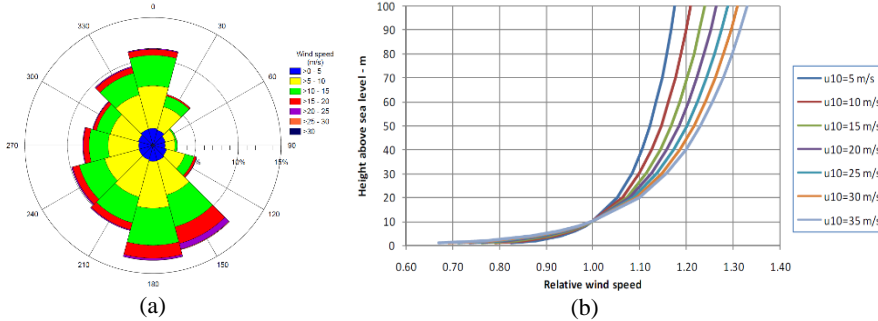


Fig. 2. (a). All-year wind rose (b) wind profiles at different wind speeds

The finite element model of the flare tower was converted into formats compatible with FRAMEWORK and USFOS for fatigue analysis. To ensure reliable comparisons, multiple cases were generated by varying key parameters. A total of 48 FRAMEWORK cases and 64 USFOS cases were analyzed, based on: Drag Factor (C_d): Values of 0.65, 1.0, 1.2, and a Reynolds number-dependent C_d , which varies with wind speed using software-defined equations. Weight Factor (W_f): Values of 0.5, 1.0, 1.1, and 1.5, applied to the structure's density to adjust mass, affecting response and natural frequency. Wind block combinations: 8, 10, and 12 wind blocks for both software, plus a 16-block case for USFOS. FRAMEWORK's 12-block limit required modifying the original 16-block scatter diagram, resulting in multiple adjusted combinations.

All cases use a full range of wind speeds and directions, weighted annually according to the scatter diagram. For the 10- and 12-block cases, higher wind speeds were added with adjusted probabilities; the 8-block case used evenly distributed wind speeds over broader ranges. The modified scatter diagrams are shown in Fig. 3.

(a)		Annual probability / wind direction													Total
wind block	m/s	0°	30°	60°	90°	120°	150°	180°	210°	240°	270°	300°	330°		
1	4	1.17	1.16	0.98	0.96	1.09	1.07	1.02	1.03	1.02	1.04	1.17	12.71		
2	8	3.59	2.55	1.44	1.33	2.03	3.03	3.72	3.27	3.01	2.79	2.75	3.28	32.79	
3	12	4.02	1.78	0.36	0.41	1.26	3.37	4.58	3.47	3.32	2.55	2.23	2.97	30.32	
4	16	2.05	0.75	0.08	0.13	0.65	2.72	2.81	1.91	1.87	1.41	0.91	1.49	16.78	
5	20	0.44	0.12	0	0.01	0.16	1.51	1.12	0.58	0.53	0.45	0.29	0.48	5.69	
6	24	0.1	0.01	0	0	0.04	0.59	0.24	0.1	0.12	0.09	0.08	0.11	1.48	
7	28	0.01	0	0	0	0.01	0.13	0.03	0.01	0.01	0	0	0.01	0.21	
8	32	0	0	0	0	0	0.01	0	0	0	0	0.01	0.01	0.02	
100.0															
(b)		Annual probability / wind direction (%)													Total
wind block	m/s	0°	30°	60°	90°	120°	150°	180°	210°	240°	270°	300°	330°		
1	4	1.17	1.16	0.98	0.96	1.00	1.09	1.07	1.02	1.03	1.02	1.04	1.17	12.71	
2	8	1.62	1.33	0.88	0.81	1.09	1.42	1.56	1.42	1.34	1.28	1.36	1.53	15.64	
3	8	1.97	1.22	0.56	0.52	0.94	1.61	2.16	1.85	1.67	1.51	1.39	1.75	17.15	
4	10	2.14	1.03	0.25	0.26	0.73	1.74	2.43	1.86	1.74	1.41	1.29	1.59	16.47	
5	12	1.88	0.75	0.11	0.15	0.53	1.63	2.15	1.61	1.58	1.14	0.94	1.38	13.85	
6	14	1.34	0.50	0.05	0.09	0.41	1.53	1.67	1.17	1.13	0.87	0.57	0.92	10.25	
7	16	0.71	0.25	0.03	0.04	0.24	1.19	1.14	0.74	0.74	0.54	0.34	0.57	6.53	
8	20	0.44	0.12	0.00	0.01	0.16	1.51	1.12	0.58	0.53	0.45	0.29	0.48	5.69	
9	24	0.10	0.01	0.00	0.00	0.04	0.59	0.24	0.10	0.12	0.09	0.08	0.11	1.48	
10	32	0.01	0.00	0.00	0.00	0.01	0.14	0.03	0.01	0.01	0.00	0.01	0.01	0.24	
100															
(c)		Annual probability / wind direction (%)													Total
wind block	m/s	0°	30°	60°	90°	120°	150°	180°	210°	240°	270°	300°	330°		
1	2	0.24	0.26	0.27	0.28	0.26	0.25	0.27	0.26	0.27	0.25	0.24	0.29	3.14	
2	4	0.93	0.90	0.71	0.68	0.74	0.84	0.80	0.76	0.76	0.77	0.80	0.88	9.57	
3	6	1.62	1.33	0.88	0.81	1.09	1.42	1.56	1.42	1.34	1.28	1.36	1.53	15.64	
4	8	1.97	1.22	0.56	0.52	0.94	1.61	2.16	1.85	1.67	1.51	1.39	1.75	17.15	
5	10	2.14	1.03	0.25	0.26	0.73	1.74	2.43	1.86	1.74	1.41	1.29	1.59	16.47	
6	12	1.88	0.75	0.11	0.15	0.53	1.63	2.15	1.61	1.58	1.14	0.94	1.38	13.85	
7	14	1.34	0.50	0.05	0.09	0.41	1.53	1.67	1.17	1.13	0.87	0.57	0.92	10.25	
8	16	0.71	0.25	0.03	0.04	0.24	1.19	1.14	0.74	0.74	0.54	0.34	0.57	6.53	
9	18	0.29	0.10	0.00	0.01	0.10	0.89	0.69	0.38	0.36	0.29	0.19	0.30	3.6	
10	24	0.25	0.03	0.00	0.00	0.10	1.21	0.67	0.30	0.29	0.25	0.18	0.29	3.57	
11	28	0.01	0.00	0.00	0.00	0.01	0.13	0.03	0.01	0.01	0.00	0.00	0.01	0.21	
12	32	0.00	0.00	0.00	0.00	0.00	0.01	0.00	0.00	0.00	0.00	0.01	0.01	0.03	
100															

Fig. 3. Regulated scatter diagrams for wind blocks (a). Eight (b). Ten, and (c). Twelve

4 Fatigue Analysis Using Power Spectral Density Method: FRAMEWORK approach

SESAM Framework uses a spectral fatigue analysis method with a hot spot stress approach based on power spectral density and S-N curve data, in accordance with standards like DNV-RP-C203 [ref], to assess fatigue life under wind buffeting loads coming from wind gusts. Overview of the process done in DNV SESAM FRAMEWORK was obtained from the user manual [8].

FRAMEWORK performs fatigue analysis using spectral methods, requiring input data such as eigenmodes, eigenfrequencies, FE model data, stress concentration factors (SCFs), and weighted wind conditions from a scatter diagram. The software generates hot spot stress power spectra at joints by decomposing the structural response into quasi-static and dynamic component.

The dynamic response is split into resonant modes, each treated as narrow-band and statistically independent, while the quasi-static response captures low-frequency effects with negligible fatigue impact. A Rayleigh distribution is assumed for stress cycles, and fatigue life is calculated using Miner's Rule with DNV T-curve S-N data for tubular joint.

Fatigue damage at each hot spot is estimated per wind state using the following sequence: (i). Spectral peaks are treated as narrow-band responses with Rayleigh-distributed stress ranges; close peaks are combined, (ii). Stress amplitude distributions are applied to S-N curves to compute damage, (iii). Damage from all peaks is summed to yield total fatigue damage. Wind input is divided into: Mean wind data, derived from the scatter diagram, gust data, characterized by power spectral density, cross-correlation functions, and probability distributions.

Wind speed at a height reference of 10 m above sea water level is used to calculate single-sided gust spectrum $S^w(f)$, where f is in cycle/s for each wind state using the NPD spectrum (for a long wind) and Panofsky spectra (for lateral and vertical components). These are combined with height profiles and cross-correlation data to calculate wind loading.

The method assumes a linear relationship between wind forcing spectra and hot spot stress spectra. Fluctuating forces on members are computed using the drag component of Morison's equation and are then mapped to nodal forces for fatigue evaluation. Once the stress transfer function between a point load and the hot spot stress is established, the hot spot stress power spectrum at each joint can be compute. The hot spot stress is first described in the time domain using Fourier transformation and the convolution theorem. By summing all forces at each master degree of freedom, the total hot spot stress spectrum at a given location is obtained.

Fatigue damage is estimated using the Palmgren-Miner rule, applying the defined S-N curve to compute annual damage across all frequency bands. The total annual damage is the sum of damage contributions from all wind states and frequency ranges.

Fatigue life is thus calculated for different load combinations, as outlined in Section 3. A total of 48 analyses were conducted in FRAMEWORK, covering three different "wind blocks" cases, four different "drag coefficient (C_d)" cases and four different "weight factor (WF)" cases. The variation in calculated fatigue lives at the most critical

joint (i.e. 101020 in Fig.1) are plotted against changes in these parameters (i.e. wind blocks= 8,10 & 12; $C_d=0.65,1.0,1.2$ & Reynold; WF=0.5,1.0,1.1 & 1.5) and results are shown in Fig. 4.

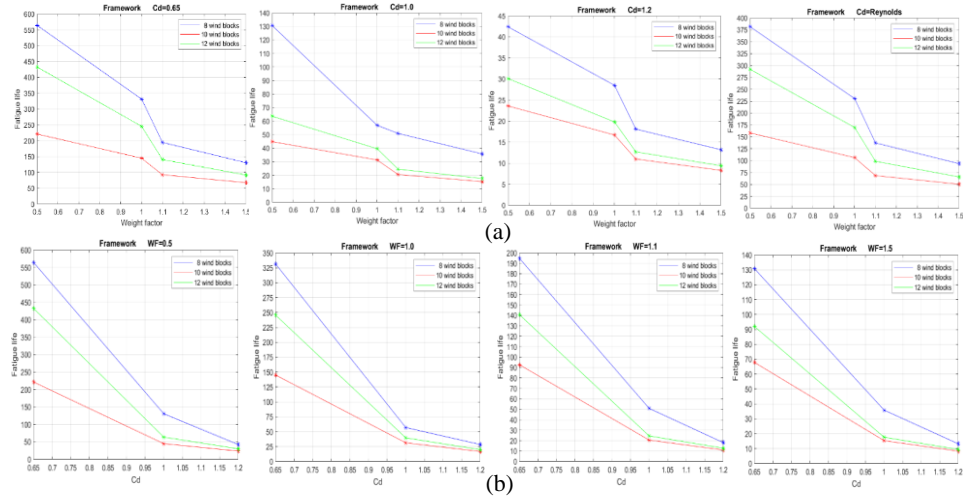


Fig. 4. Fatigue life (FRAMEWORK method) variation for different wind blocks with (a). weight factor, WF values (b). drag coefficient, C_d values

5 Fatigue Analysis using Time Domain Method: USFOS approach

USFOS is used to perform a full nonlinear dynamic analysis of the flare boom under the effects of wind buffeting. The dynamic analysis accounts for both geometric and load nonlinearities resulting from the deflective response of members at each time step.

5.1 Decision of time increment for time history analysis

A smaller time increment increases accuracy but also demands more computation time and storage. To balance accuracy and efficiency, analyses were run using time increments of 0.02, 0.05, 0.10, 0.20, and 0.50 seconds. Fatigue life improved significantly as the time increment decreased, particularly for the larger steps. The difference between 0.02 and 0.05 seconds was negligible, while the 0.02-second analysis took twice as long to run. Using 0.05 seconds instead of 0.10 seconds roughly doubled the estimated fatigue life. Thus, 0.05 seconds was chosen for the final analysis as it offers a good balance between accuracy and computational cost.

5.2 Structural analysis and fatigue life assessment

The load cases correspond to the mean wind speeds, directions, and associated probabilities as represented in the scatter diagram (refer to figure). Each wind speed is simulated with time-varying wind input to capture the wind buffeting effect. The wind fields

are derived from site-specific Metocean data. To account for wind directionality, the structural model is rotated by the directional interval (30°) as defined in the scatter diagram. Each case involves a combination of a wind field and the corresponding rotated structural model. The outputs of the nonlinear analysis are stress time series for each critical joint (i.e nodes in the FE model).

FATAL is used to process the output files and convert the stress time series into stress ranges using the rainflow counting method. Stress concentration factors (SCFs) are applied as input and multiplied at the relevant hot spots. These hotspot stresses, along with the DNV T-air S-N curve and Palmgren-Miner's rule, are used to estimate fatigue damage.

FATAL POST scales down damage from each load case by multiplying correlating annual probability from the scatter diagram. Finally, the fatigue damage from all load cases is summed and sorted from highest to lowest for each node.

Fatigue life is thus calculated for different load combinations, as outlined in Section 3. A total of 64 analyses were conducted in USFOS, covering four different "wind blocks" cases, four different "drag coefficient (C_d)" cases and four different "weight factor (WF)" cases. The variation in calculated fatigue lives at the most critical joint (i.e. 101020 in Fig.1) are plotted against changes in these parameters (i.e. wind blocks= 8,10,12 & 16; C_d =0.65,1.0,1.2 & Reynold; WF=0.5,1.0,1.1 & 1.5) and results are shown in Fig. 5.

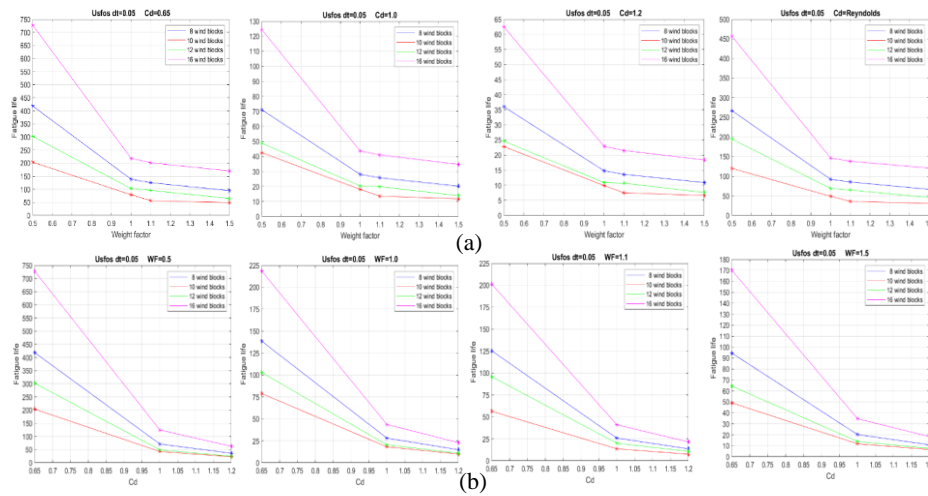


Fig. 5. Fatigue life (USFOS method) variation for different wind blocks with (a). weight factor, WF values (b). drag coefficient, C_d values

5.3 Relative velocity

Relative velocity is a phenomenon that primarily affects structures with large motions, such as wind turbines. USFOS includes a built-in function that accounts for this phenomenon through wind forces, as described in DNV RP-C205 [8]. To investigate the effect of this function on slender structures, eight full fatigue analyses were conducted in USFOS as part of the case study.

On average, the use of this formula in above mentioned DNV RP-C205 resulted in a 196% increase in fatigue life (i.e., approximately three times longer) compared to analyses that excluded it. This represents a drastic reduction in damage, which is considered unlikely, as real-world relative velocity is unlikely to have such a significant impact on wind-induced loading in rapidly moving slender structures. As noted in DNV RP-C205 [8]: “Relative velocity may lead to an over-estimation of damping if the displacement is less than the member diameter.”

The approach used in section 4 (i.e. FRAMEWORK approach) is based on static analysis and therefore does not include a relative velocity function. As a result, relative velocity is not considered in the main analyses and comparisons. However, the results suggest that caution should be exercised when applying this function to rapidly moving slender structures, as it may lead to an underestimation of fatigue damage.

6 Summary of the results and comparison

The main objective in this section is to compare fatigue life estimates from two software tools, which differ in their assessment methods: Framework uses the spectral density method, while USFOS employs a nonlinear dynamic time/stress history approach. The variation in calculated fatigue lives from both methods at the most critical joint (i.e. 101020/ 159 in Fig.1) are plotted against changes in considered parameters (i.e. wind blocks= 8,10,12 & 16; $C_d=0.65,1.0,1.2$ & Reynold; WF=0.5,1.0,1.1 & 1.5) and results are compared in Fig. 6. USFOS analysis of time increment 0.05 seconds is also more accurate and gives more conservative results than the analysis with time increment of 0.1 seconds. The obtained fatigue lives of most critical joint (i.e. 101020/ 159 in Fig.1)

6.1 Overall comparison

On average, USFOS predicts 66% of the fatigue life estimated by FRAMEWORK. For cases with a weight factor of 1.0, USFOS predicts only 49%. Determining which software is more accurate is challenging due to numerous assumptions and limited real-world fatigue data for similar structures.

A key difference between the two tools is the identification of the most critical joint. These do not align, instead, they are mirrored counterparts. This may stem from how each software handles wind direction data. USFOS distributes probabilities over a full 360° wind rose, while FRAMEWORK uses a half-circle with combined opposing directions. Because the actual wind distribution is not symmetrical, this leads to differences in accumulated fatigue damage.

FRAMEWORK mirrors load across the structure, which may be reasonable for symmetrical geometries, but not for asymmetrical ones. In this case study, with a partially symmetrical structure, FRAMEWORK misidentified the critical node. Without the USFOS analysis, this might have gone unnoticed. All plots in Fig. 6 show that fatigue life is more sensitive to changes in C_d when $C_d < 1$. This is expected, as C_d directly affects wind-induced forces, and due to the logarithmic nature of the S–N curve, higher stresses lead to greater sensitivity.

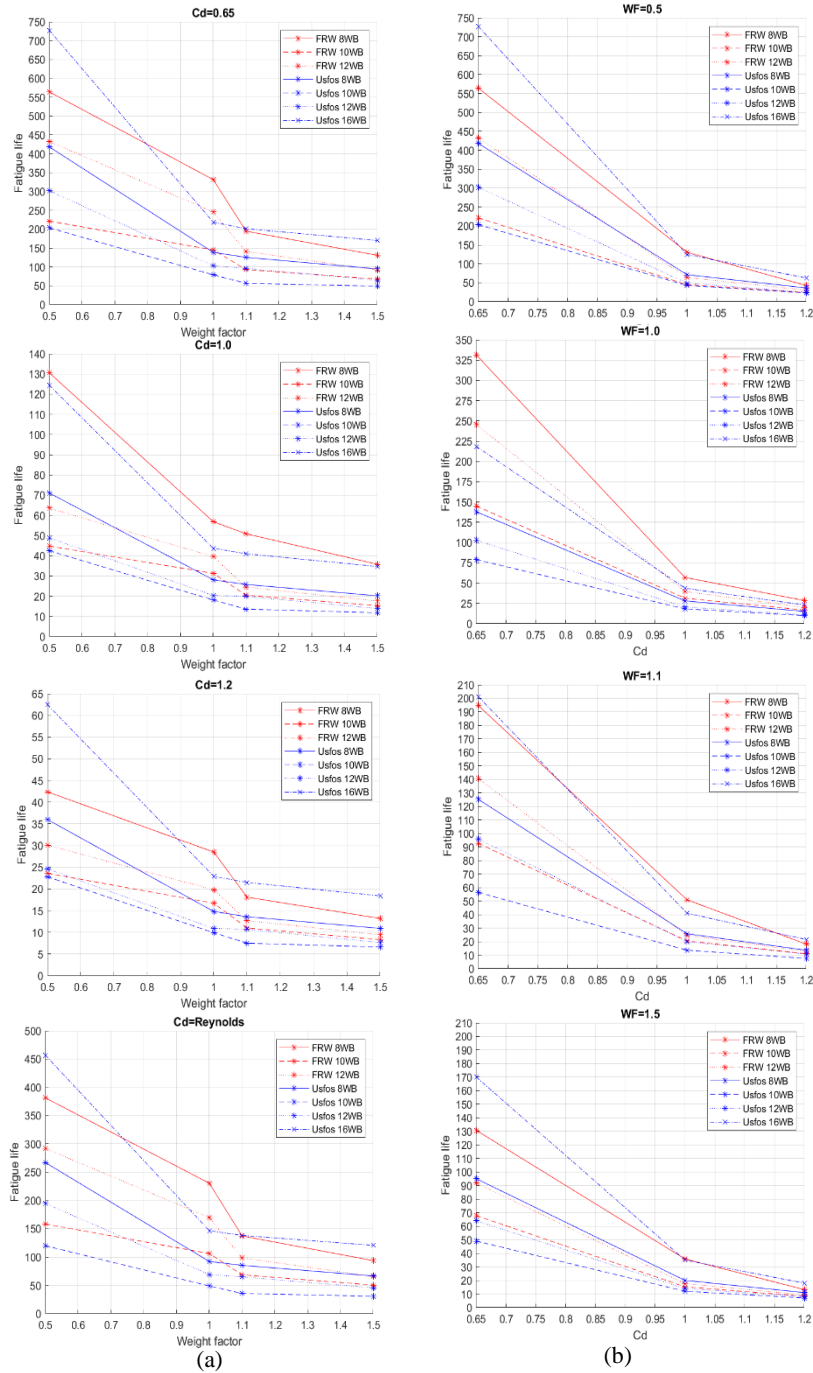


Fig. 6. Comparison of fatigue lives (from both FRAMEWORK & USFOS) for different wind blocks with (a). weight factor, WF values (b). drag coefficient, C_d values

6.2 Sensitivity of wind blocks

A general trend shows that the 8-wind-block case yields the highest fatigue life, while the 10-wind-block case results in the lowest. On average, fatigue life in the 12-wind-block case is 68% lower than in the 8-wind-block case in FRAMEWORK, and 49% lower in the 10-wind-block case. Although the 10- and 12-block cases include more wind blocks, they combine higher wind speeds over longer ranges (see chapter), which significantly impacts fatigue life despite the low probability of these extreme winds. The obtained fatigue lives of most critical joint (i.e. 101020/ 159 in Fig.1) for 10-wind-block case is shown in Table 1.

This is expected, as fatigue damage increases exponentially with stress. Therefore, for accurate fatigue assessment, high wind speeds should be prioritized to avoid overly conservative results. In contrast, wider ranges may be used for low wind speeds, as their impact on fatigue is minimal. If software like FRAMEWORK limits the number of wind blocks, grouping high wind speeds can lead to overly conservative estimates. To optimize fatigue prediction, lower wind speeds should be grouped instead.

6.3 Sensitivity of natural frequency

The structural model appears equally sensitive to changes in weight factor across both software tools. Increased mass lowers the natural frequency, bringing it closer to the fluctuating frequency of wind, which amplifies resonant motion. Although higher mass typically implies greater inertia and reduced movement, the slenderness of the structure allows oscillations to persist. Instead of damping vibrations, the added mass seems to worsen stress conditions and increase fatigue damage.

Fatigue damage increases sharply in all FRAMEWORK analyses when the weight factor rises from 1.0 to 1.1, with an average 36% increase. This likely reflects a shift in natural frequency toward a dominant peak in the wind spectrum. Beyond this point, sensitivity decreases as the frequency moves past the peak.

USFOS shows a more linear relationship between fatigue damage and weight factor, indicating less sensitivity to specific frequencies. This is expected, as its time-series approach captures the wind's random fluctuations more realistically than the spectral method used in FRAMEWORK, which lacks dynamic response. While USFOS is based on wind spectra and should theoretically resemble the spectral approach, its dynamic analysis introduces greater variability. In contrast, the spectral method assumes more constant loading by transferring wind energy to stress spectra, isolating stress bands, and summing damage.

Both methods rely on Miner's rule, which assumes that variable stress cycles have the same fatigue effect as constant amplitude cycles of equal magnitude. This is similar to the narrow-band assumption in FRAMEWORK, which can lead to inaccurate damage accumulation prediction. Because FRAMEWORK involves a double constant-amplitude assumption, it is more sensitive to specific frequencies. USFOS better captures fluctuating stresses through dynamic analysis and applies Miner's rule only during the stress-to-damage conversion.

Table 1. Fatigue life for most critical joint of the flare boom for 10-wind-block case

Drag coefficient (C_d)	Weight factor (WF)	Fatigue life (years)		
		FRAMEWORK	USFOS dt=0.05	USFOS dt=0.10
0.65	0.5	221	204	576
	1.0	145	79	116
	1.1	93	56	149
	1.5	68	49	87
1	0.5	45	43	114
	1.0	31	18	27
	1.1	20	14	33
	1.5	15	12	20
1.2	0.5	24	23	60
	1.0	17	10	15
	1.1	11	8	18
	1.5	8	7	11
Reynold's	0.5	158	120	313
	1.0	106	49	69
	1.1	69	36	91
	1.5	50	31	55

7 Conclusions

Two fatigue life estimation methods were compared with a case study flare boom: the spectral density approach (FRAMEWORK) and the time history approach (USFOS). Both used the same structural model, focusing on the most critical joint. A parametric study compared sensitivity to changes in structural weight, drag coefficient, wind block configuration, and relative velocity. The impact of time increment was also assessed in USFOS but not treated as a parameter, as an appropriate increment must always be used and is case dependent. The key findings/conclusions of this comparative study are listed below.

- *Software differences:* FRAMEWORK is easier to set up with less input required. USFOS requires simulated wind fields but offers better error detection and full stress history output, providing greater control and validation. FRAMEWORK, relying on spectral estimates, offers less control.
- *Wind blocks effect:* More wind blocks generally result in longer predicted fatigue life due to less conservative rounding. In USFOS, 16 wind blocks lead to a 66% increase in fatigue life compared to 8 blocks. However, for 10 and 12 blocks, longer-duration high wind speeds reduce fatigue life to 54% and 73% (10 and 12 blocks, respectively) in USFOS and 49% and 68% in FRAMEWORK, relative to the 8-block case
- *Resonance effects:* FRAMEWORK-generated wind spectra may align peak energy with the natural frequency at weight factor 1.1, potentially causing resonance. USFOS, using time histories, is less sensitive to frequency alignment, possibly explaining the lower impact at this weight factor.

- *Drag coefficient (C_d):* In USFOS, changes in C_d alter stress magnitudes but not patterns. Stress differences match the proportional changes in C_d , indicating a direct relationship between C_d and stress.
- *Fatigue life estimates:* USFOS predicts shorter fatigue life than FRAMEWORK, on average, 66% from FRAMEWORK estimated life across all cases, dropping to 49% for weight factor 1.0. The accuracy of both methods requires experimental validation.

Further study is recommended to better understand the limitations and accuracy of both methods. Experimental validation is necessary to further confirm their accuracy and reliability for engineering applications.

Acknowledgement

Authors highly appreciate Aker Solutions and Ådne Hausberg, Department Manager for the opportunity and tools to pursue this study. We also appreciate Tore Holmås and Anders Holstad for their support with USFOS and remote guidance. Authors acknowledge ChatGPT for assistance with English proof reading.

References

1. DNV: Environmental Conditions and Environmental Loads (RP-C205). DNV AS, September (2019)
2. Saini, D.D.S., Kim-Chew, D.: A review of stress concentration factors in tubular and non-tubular joints for design of offshore installations. J. Ocean Eng. Sci., Kanpur (2016)
3. Jia, J., Edge, R., Johnson, E.: The Effects of Wind Modeling Considerations and Wind Direction on an Accurate Fatigue Life Assessment. Int. Soc. Offshore Polar Eng. (2010)
4. Fuštar, B., Lukić, I.: Review of Fatigue Assessment Methods for Welded Steel Structures. Adv. Civ. Eng. (2018)
5. Naess, A., Moan, T.: Stochastic Dynamics of Marine Structures. Cambridge University Press, New York (2013)
6. American Petroleum Institute (API): API RP 2A-WSD: Recommended Practice for Planning, Designing and Constructing Fixed Offshore Structures – Working Stress Design, 21st edn. API, with Errata and Supplements (2002, 2005, 2007)
7. DNV: Fatigue Design of Offshore Steel Structures (RP-C203). DNV AS (2019)
8. DNV GL: Framework User Manual. DNV GL AS (2020)